

1 **Supporting Information**

2 **In Situ Hg²⁺ Improved Peroxidase-like Activity and Triggered “on”**
3 **Oxidase-like Activity of Yolk-shell Co₃S₄ Microspheres for Detection**
4 **of Hg²⁺**

5
6 **Kang Qin^b, Ying Chu^b, Chang Xu^b, Guijiang Li^b, Xixi Zhu^b, Gaochao Fan^c**
7 **Zhongdong Yang^{a,*} and Qingyun Liu^{b,*}**

8
9 *^a Shandong University of Science and Technology Hospital, Shandong University of*
10 *Science and Technology, Qingdao 266590, China*

11 *^b College of Chemical and Biological Engineering, Shandong University of Science*
12 *and Technology, Qingdao 266590, China*

13 *^c Shandong Key Laboratory of Biochemical Analysis, College of Chemistry and*
14 *Molecular Engineering, Qingdao University of Science and Technology, Qingdao*
15 *266042, China*

16 *** Corresponding Author**

17 E-mail: skd994016@sdust.edu.cn (Z. Yang); qyliu@sdust.edu.cn(Q. Liu)

18 Tel: +86 0532 86057757

19 **Number of pages: 14**

20 **Number of Figures: 11**

21 **Number of Tables: 2**

22 **Number of Videos: 1**

23 **Associated Content**

24 Experimental Section (Materials, Instruments, Preparation of Co_3S_4 yolk-shell
25 microspheres, Assay of the peroxidase-like activity of Co_3S_4 , Steady-state kinetics,
26 Assay of the oxidase-like activity, Assay of detection of Hg^{2+});
27 XRD pattern of Co_3S_4 microspheres (a), SEM image of precursor (b), SEM image of
28 Co_3S_4 (c), and TEM image of Co_3S_4 (d) (Fig. S1);
29 BET data of Co_3S_4 yolk-shell spheres (Fig. S2);
30 Assay of catalytic activity of Co_3S_4 (Fig. S3);
31 (a) Assay of the peroxidase-like activity of Co_3S_4 , (b) Fluorescence intensity, (c) and
32 (d) ESR data of Co_3S_4 (Fig. S4);
33 Assay of the oxidase-like activity of Co_3S_4 (Fig. S5);
34 Steady-state kinetic (Fig. S6);
35 Assay of the oxidase-like activity (Fig. S7);
36 TEM image of $\text{HgS}/\text{Co}_3\text{S}_4$ (a), XRD data of Co_3S_4 and $\text{HgS}/\text{Co}_3\text{S}_4$ (b), and TEM-EDX
37 mapping images of $\text{HgS}/\text{Co}_3\text{S}_4$ (c) (Fig. S8);
38 XPS spectra of Co_3S_4 and $\text{HgS}/\text{Co}_3\text{S}_4$ (Fig. S9);
39 (a) and (b) Assay of the oxidase-like activity, (c) ESR data of $\text{HgS}/\text{Co}_3\text{S}_4$ (Fig. S10);
40 Selectivity of sensor (Fig. S11);
41 Comparison of K_m (Table S1);
42 Comparison of Hg^{2+} detection (Table S2);
43 Color changes of the reaction systems in the presence of Hg^{2+} or in the absence of
44 Hg^{2+} (Video S1).

45 **Experimental Section**

46 **Materials**

47 HgCl₂, thioacetamide (TAA) and 3,3',5,5'-tetramethylbenzidine dihydrochloride
48 (TMB) were commercially purchased from Macklin (Shanghai, China).
49 Fe(NO₃)₃•9H₂O, Co(NO₃)₂•6H₂O, NaCl, KCl, MgSO₄, H₂O₂ (30 wt%), Terephthalic
50 acid, disodium ethylenediaminetetraacetic acid (EDTA-2Na), Lactose (Lac), D-
51 histidine (Hi), isopropanol (IPA), p-benzoquinone (PBQ), Dserine (Ser), L-arginine
52 (Arg), and Sucrose (Suc) were obtained from Sinopharm Chemical Reagent Co., Ltd.
53 (Shanghai, China).

54 **Instruments**

55 The surface state of elements and the phase of Co₃S₄ yolk-shell microspheres
56 were systematically characterized by X-ray photoelectron spectroscopy (XPS,
57 Thermo ESCALAB 250Xi, USA) and X-ray diffractometer (Cu-K α radiation, 2 θ =
58 10-80°, 5°/min), respectively. The morphology was investigated by the transmission
59 electron microscope with the energy dispersive X-ray spectroscopy (TEM, FEI,
60 APREO, USA). Fluorescent spectra and UV–vis absorption spectra were recorded on
61 a fluorescence spectrophotometer (FL, Hitachi F-4600, Japan) and a UV-8000PC
62 spectrophotometer (Puxi, TU 1810, China), respectively. The Bru-nauer-Emmett-
63 Teller surface were analyzed on a Micromeritics ASAP 2460 at 77.3 K.

64 **Preparation of Co₃S₄ yolk-shell microspheres**

65 In a typical synthesis process, 0.2734 g Co(NO₃)₂•6H₂O were dissolved in the
66 mixed solvents glycerol (7.5 mL) and isopropanol (52.5 mL) resulting a clear pink

67 solution. The formed mixture was then transferred into Teflon-sealed autoclave and
68 heated at 150 °C for 24 h. Natural cooling to room temperature, the purple precipitate
69 was obtained via centrifugation, rinsed with absolute ethanol six times and dried at 60
70 °C.

71 For the synthesis of hollow Co_3S_4 yolk-shell microspheres, 0.0300 g purple
72 precipitate was dispersed into 20.0 mL ethanol solution including 0.0500 g
73 thioacetamide (TAA). Then, the resulting solution was sealed in Teflon-sealed
74 autoclave and performed at 180 °C for 12 h. After centrifugation and rinsed with
75 distilled water and ethanol several times, the hollow Co_3S_4 coreshell nanospheres
76 were finally synthesized.¹

77 **Assay of the peroxidase-like activity of Co_3S_4**

78 Typically, 200 μL of Co_3S_4 aqueous suspension, 200 μL of H_2O_2 and 200 μL of
79 TMB were added into 1400 μL buffer solution in turn, and the absorbance at 652 nm
80 was recorded after reaction for 2 min. The optimal catalytic conditions of the Co_3S_4
81 nanozyme were evaluated by tuning pH values of buffer solutions as well as the
82 various temperatures.

83 **Steady-state kinetics**

84 The catalytic kinetics of Co_3S_4 dual nanozymes was studied by changing the
85 concentration of the substrates TMB or H_2O_2 , and keep the other unchanged,
86 respectively. Herein, the kinetic study was carried out using 200 μL of Co_3S_4
87 microspheres (0.3 mg/mL) in a reaction volume of 200 μL with 0.1 mM TMB or 25
88 mM H_2O_2 . K_m and V_{\max} were calculated by the double reciprocal graph of the

89 Michaelis-Menten equation, that is, $1/v = (K_m/V_{max}) \times (1/[S]) + 1/V_{max}$, where V_{max}
90 and v represent the maximum reaction velocity and initial speed, as well as $[S]$ and
91 K_m represent the substrate concentration and Michaelis constant, respectively.

92 **Assay of the oxidase-like activity**

93 Briefly, 200 μL of Co_3S_4 , 200 μL of Hg^{2+} and 200 μL of TMB were added into
94 1400 μL buffer solution reacted for 2 min, and the absorbance at 652 nm was
95 recorded. Similar to the study of peroxidase-like activity of Co_3S_4 , it was necessary to
96 study the influences of the experimental temperatures and pH values on the oxidase-
97 like activity.

98 **Assay of detection of Hg^{2+}**

99 **Colorimetric Hg^{2+} detection based on the peroxidase-like activity of Co_3S_4**

100 Firstly, different concentrations of Hg^{2+} (200 μL) and peroxidase-like nanozyme
101 Co_3S_4 (200 μL , 0.3 mg/mL) were added to HAc-NaAc buffer (pH = 4) and incubated
102 at room temperature for 2 min. Then, add H_2O_2 (1 mM, 200 μL) together with TMB
103 (0.1 mM, 200 μL) into the above mixture reacted for 2 min and report the absorbance
104 at 652 nm.

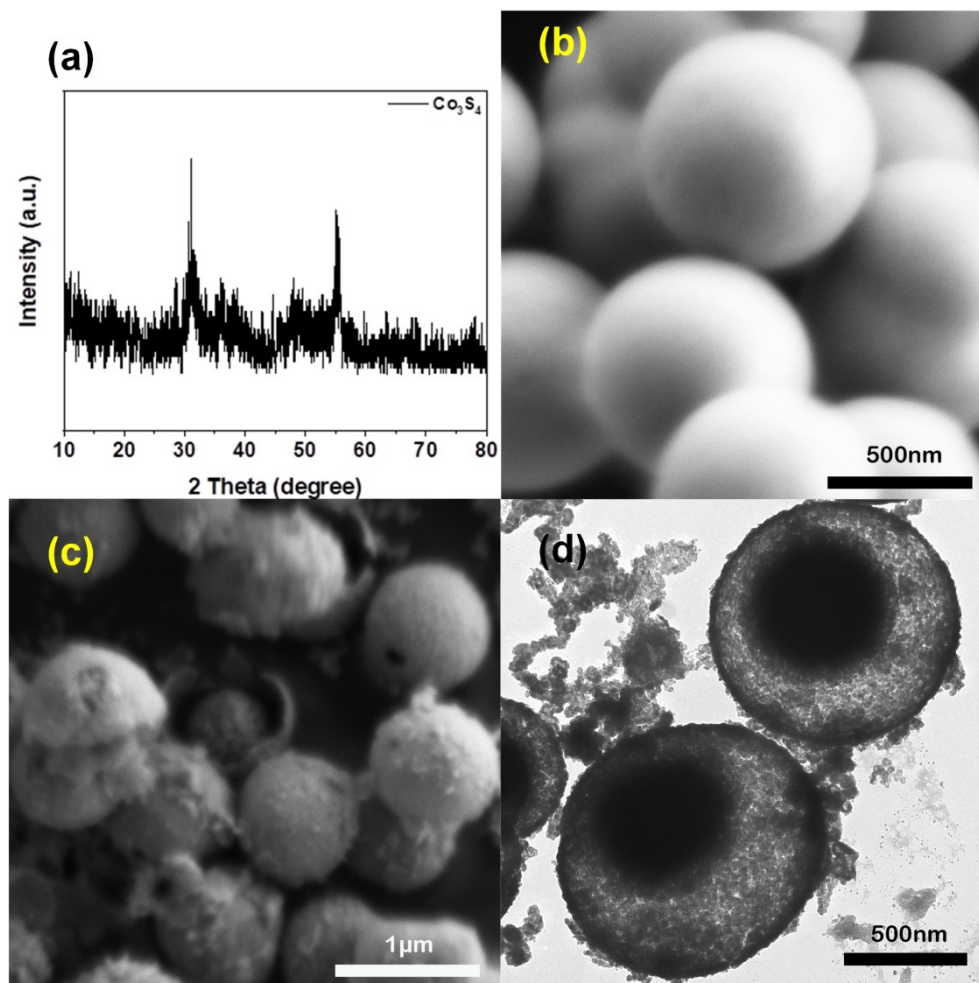
105 **Colorimetric Hg^{2+} detection based on the oxidase-like activity of Co_3S_4**

106 Different concentrations of Hg^{2+} (200 μL), Co_3S_4 (200 μL , 0.3 mg/mL) and TMB
107 (0.1 mM, 200 μL) were added into HAC-NaAC buffer (pH = 5), which was incubated
108 at room temperature for 2 min. Then, the absorbance at 652 nm was reported.

109 **XPS spectra of $\text{HgS}/\text{Co}_3\text{S}_4$**

110 From Fig. S9a, the elements Hg, Co, and S are detected in the final production

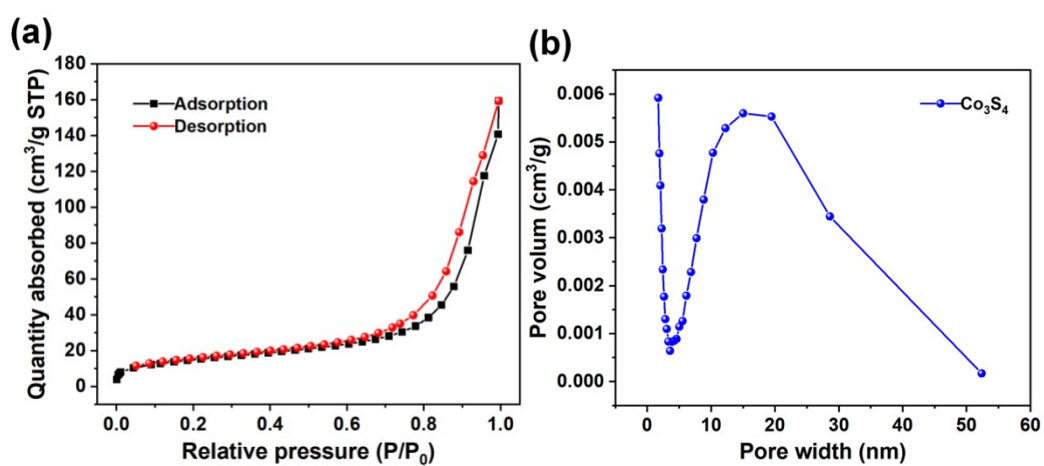
111 HgS/Co₃S₄. The Co 2p peak in HgS/Co₃S₄ shows a positive shift of 1.0 eV due to the
112 influence of the introduced Hg²⁺ (Fig. S9b). The typical peaks centered at 161.4 and
113 162.2 eV are S 2p_{1/2} and S 2p_{3/2}, respectively, indicating that the oxidation state of
114 S²⁻ exists in Co₃S₄ (Fig. S9c). ² For HgS/Co₃S₄, a decrease in the main peak at 165.9
115 eV is detected (Fig. S9c), indicating the influence of the produced HgS. In addition, as
116 seen from Fig. S9d, two peaks at 100.22 and 104.22 eV in HgS/Co₃S₄ indicate that Hg
117 mainly exists in the 2+ oxidation state. ³ Thereof, it can be suggested that the
118 produced HgS is attached to Co₃S₄ subsequently.



120

121 **Fig. S1** XRD pattern of Co_3S_4 microspheres(a); SEM image of precursor (b); Images of SEM (c)

122 and TEM (d) of yolk-shell Co_3S_4

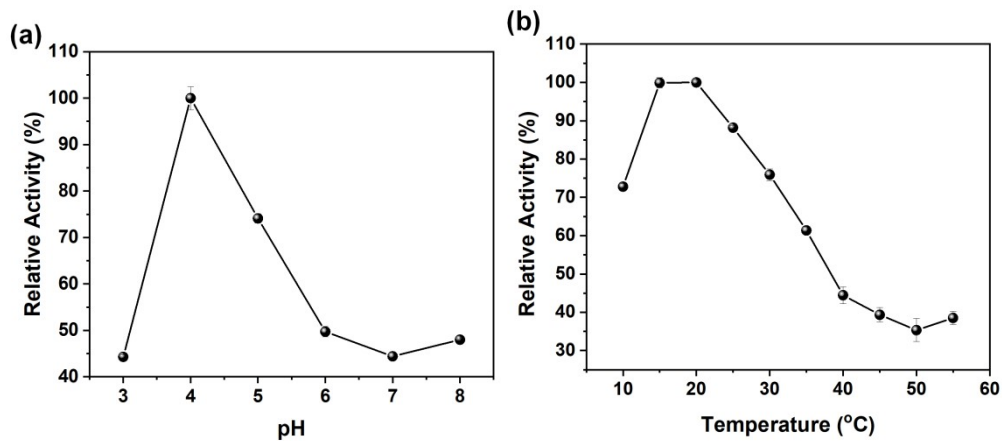


123

124 **Fig. S2** N_2 adsorption/desorption isotherms (a) and the pore volume (b) of Co_3S_4 yolk-shell

125 spheres.

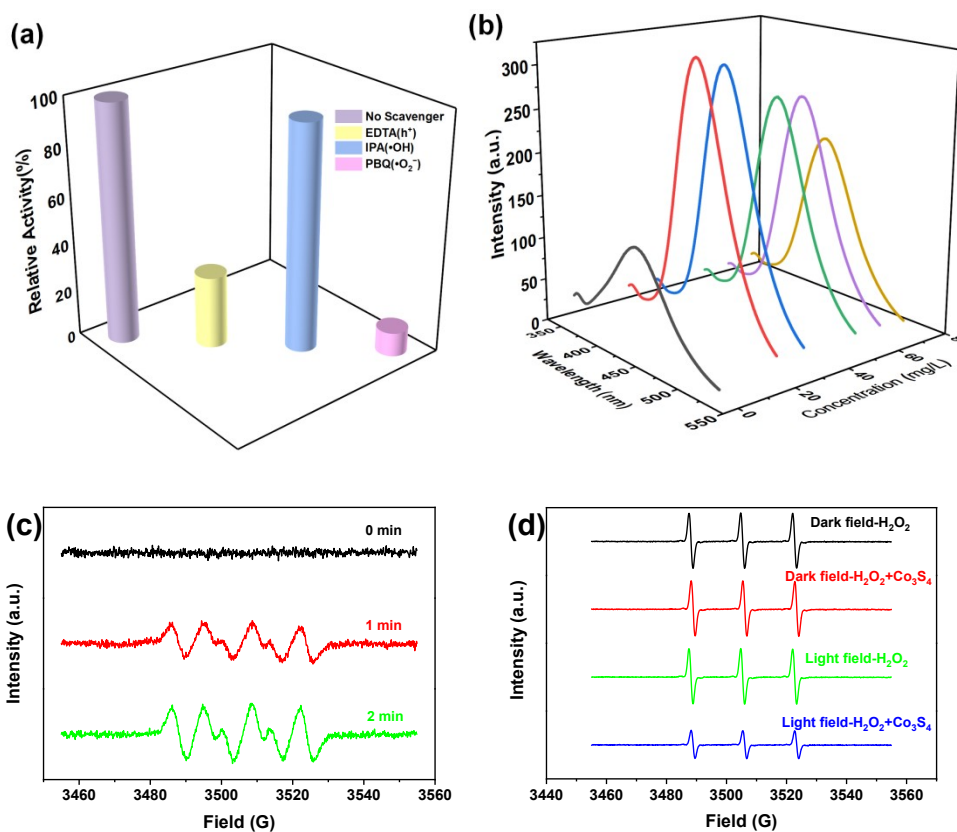
126



127

128 **Fig. S3** Influences of the catalytic activity of Co_3S_4 on pH (a) and temperature (b), respectively.

129



130

131

132 **Fig. S4** (a) Effects of various active scavengers during the catalytic oxidation of TMB by Co_3S_4

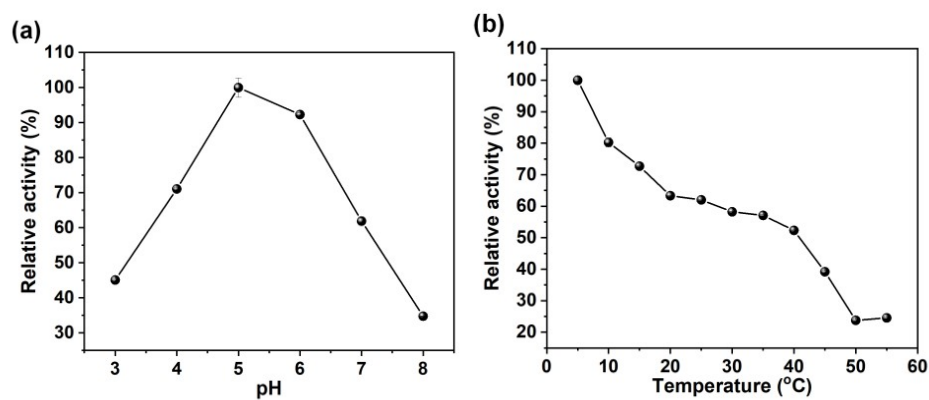
133 under natural light. (b) Fluorescence intensity varies with the amount of Co_3S_4 . Fluorescent tests:

134 Co_3S_4 as catalyst, H_2O_2 24 mM, TA 0.5 mM, pH of 4, 20 °C, 30 min. (c) Generation of $\cdot\text{O}_2^-$ by

135 Co_3S_4 nanozymes in the presence of 1mM H_2O_2 (methanol system), and (d) photogenerated hole

136 in water system.

137

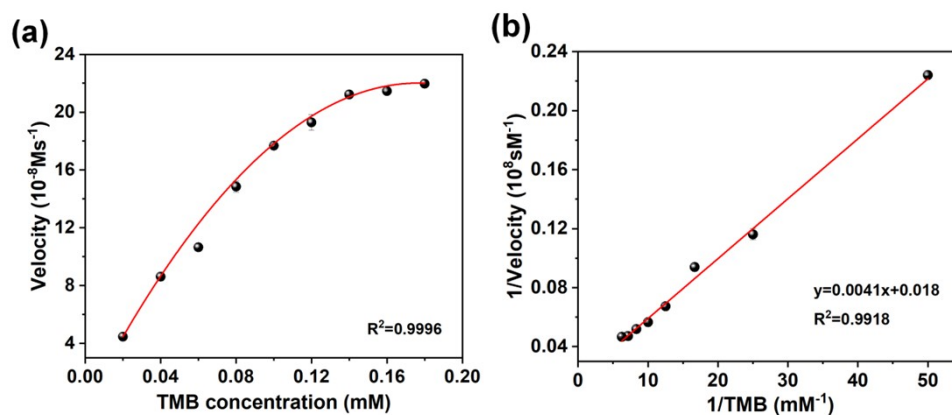


138

139 **Fig. S5** Influences of pH (a) and temperature (b) on the oxidase-like activity of Co_3S_4 ,

140 respectively.

141



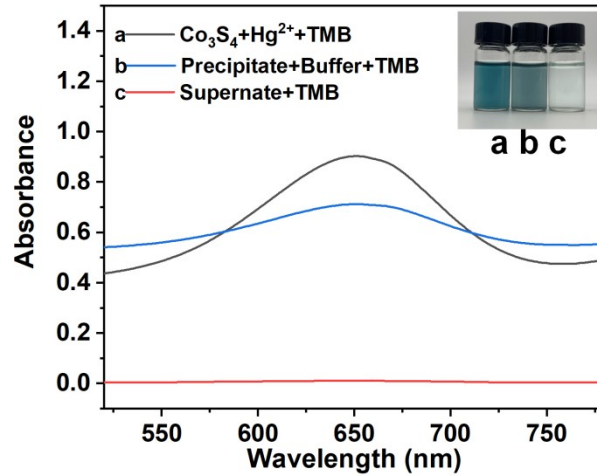
142

143 **Fig. S6** Steady-state kinetic assay of Hg^{2+} triggered “ON” Co_3S_4 oxidase-like activity by (a)

144 varying the concentrations of TMB from 20 to 200 μM with a fixed amount of Hg^{2+} (1 mM) (b) is

145 corresponding double reciprocal curve towards TMB.

146

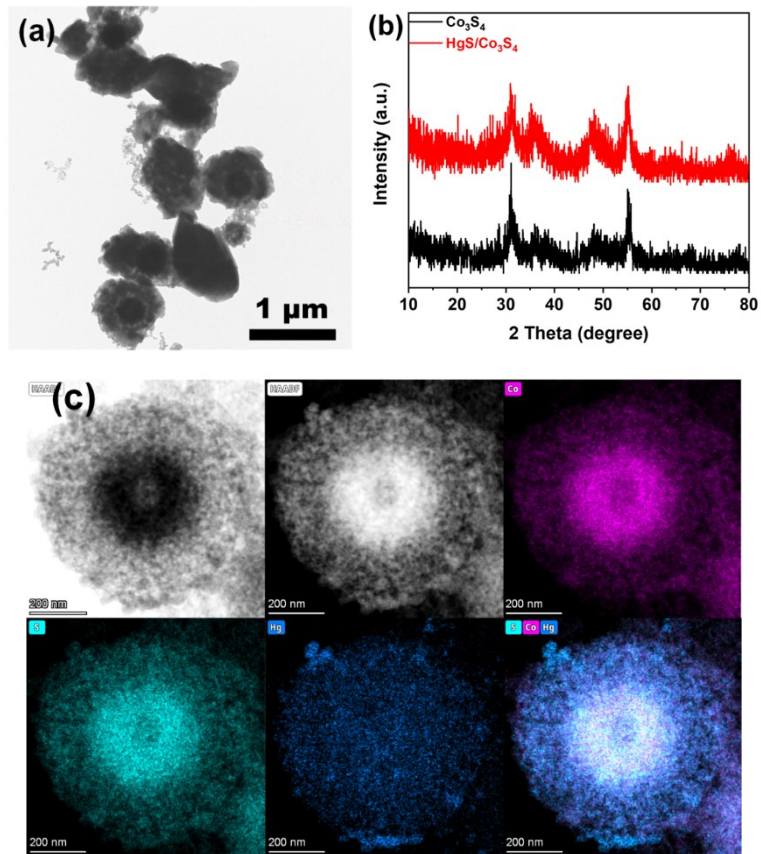


147

148 **Fig. S7** Comparison of the oxidase-like activity whether precipitate ($\text{HgS}/\text{Co}_3\text{S}_4$) or supernate

149 taken from the reaction system after Hg^{2+} mixed with Co_3S_4 under natural light.

150

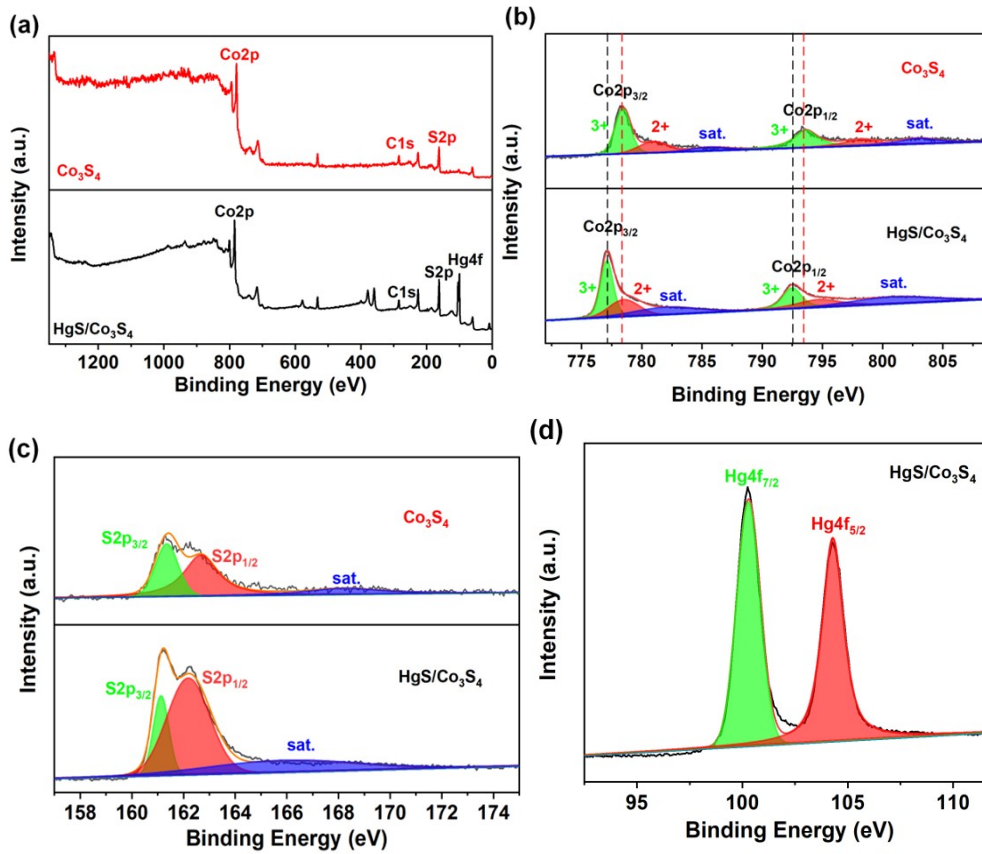


151

152

153 **Fig. S8** TEM image of $\text{HgS}/\text{Co}_3\text{S}_4$ (a), XRD data of Co_3S_4 and $\text{HgS}/\text{Co}_3\text{S}_4$ (b), and TEM-EDX

154 mapping images of $\text{HgS}/\text{Co}_3\text{S}_4$ (c), respectively.



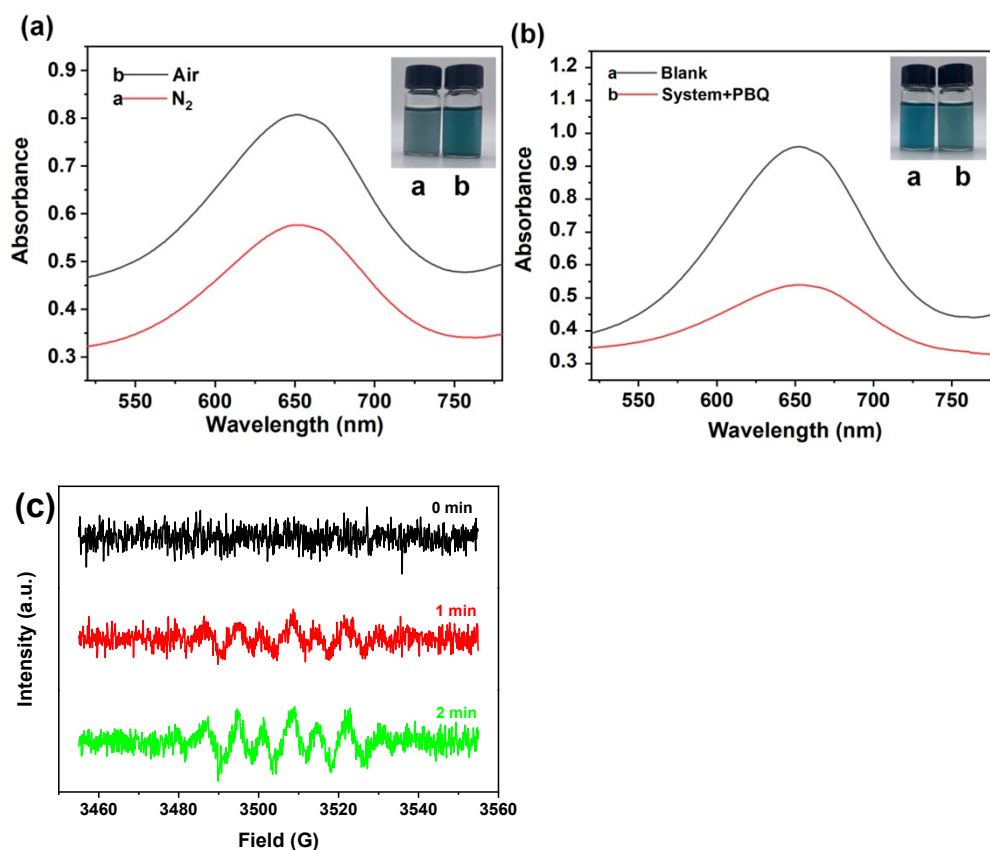
155

156

157 **Fig. S9** High-resolution XPS spectra of Co_3S_4 and $\text{HgS}/\text{Co}_3\text{S}_4$: survey (a), Co 2p (b), S 2p (c) and

158 Hg 4f (d), respectively.

159



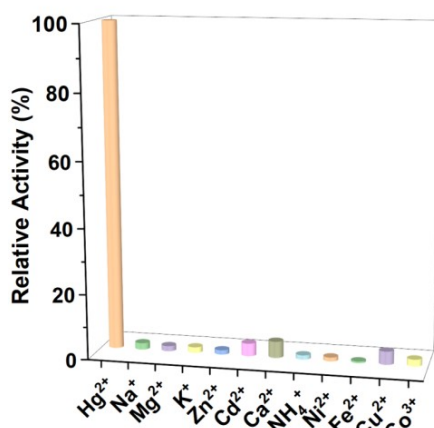
160

161

162 **Fig. S10** (a) The influences on the oxidase-like activity of Hg-Co₃S₄ under air-saturated or N₂-
 163 saturated conditions (inset: the corresponding photographs); (b) In the presence or absence of PBQ.

164 (c) Generation of •O₂⁻ by HgS/Co₃S₄ without the presence of H₂O₂ (methanol system).

165



166

167 **Fig. S11** The selectivity of the Co₃S₄-based sensor towards Hg²⁺ (1.0 mM) in the presence of
 168 interferents (100 mM).

170 **Table S1** Comparison of K_m of nanozymes towards TMB substrate.

Nanozymes	K_m /mM	Ref.
Co-V MMO (oxidase)	0.44	4
CeO ₂ (oxidase)	0.80	5
Selenium (oxidase)	8.30	6
Co ₃ S ₄ (peroxidase)	0.82	This work
Co ₃ S ₄ -Hg ²⁺ (oxidase)	0.22	This work

171

172 **Table S2** Comparison of Hg²⁺ detection based on Hg²⁺-triggered Co₃S₄ oxidase-like activity with
173 the previous studies.

Nanozymes	LOD (nM)	Ref.
GO-Ag (fluorimetric)	590	7
Ag/GO (colorimetric)	338	8
p-PDA/Ag(colorimetric)	800	9
Ficuscaricastem-Ag(colorimetric)	1060	10
Co ₃ S ₄ (peroxidase)	170	This work
Co ₃ S ₄ -Hg ²⁺ (oxidase)	55	This work

174



video.mp4

175

176 **Video S1** Color changes of the reaction systems in the presence of Hg²⁺ or in the absence of Hg²⁺.

177 **Left system:** Buffer solution (pH = 4), Co₃S₄ (0.3 mg/L), TMB (1 mM) and Hg²⁺ (1 mM).

178 **Right system:** Buffer solution (pH = 4), Co₃S₄ (0.3 mg/L) and TMB (1 mM).

179

180 **References**

- 181 1. L. Shen, L. Yu, H. B. Wu, X.-Y. Yu, X. Zhang and X. W. Lou, *Nature Communications*, 2015, **6**.
- 182 2. H. Chen, J. Jiang, L. Zhang, H. Wan, T. Qi and D. Xia, *Nanoscale*, 2013, **5**, 8879-8883.
- 183 3. J. S. Lee, M. S. Han and C. A. Mirkin, *Angew Chem Int Ed Engl*, 2007, **46**, 4093-4096.

- 184 4. Y. Wang, C. Chen, D. Zhang and J. Wang, *Applied Catalysis B: Environmental*, 2020, **261**.
- 185 5. A. Asati, S. Santra, C. Kaittanis, S. Nath and J. M. Perez, *Angew Chem Int Ed Engl*, 2009, **48**,
186 2308-2312.
- 187 6. L. Guo, K. Huang and H. Liu, *Journal of Nanoparticle Research*, 2016, **18**.
- 188 7. S. D. Hiremath, K. K. Maiti, N. N. Ghosh, M. Banerjee and A. Chatterjee, *ACS Applied Nano*
189 *Materials*, 2020, **3**, 3071-3079.
- 190 8. A. Syed, N. Marraiki, S. Al-Rashed, A. M. Elgorban and M. T. Yassin, *Spectrochim Acta A Mol*
191 *Biomol Spectrosc*, 2021, **244**, 118844.
- 192 9. A. Kalam, A. G. Al-Sehemi, S. Alrumman, M. Assiri, M. F. M. Moustafa, P. Yadav and M.
193 Pannipara, *Green Chemistry Letters and Reviews*, 2018, **11**, 484-491.
- 194 10. S. A. Pande, B. Pandit and B. R. Sankapal, *Materials Letters*, 2017, **209**, 97-101.
- 195